

액주를 이용한 충격파 완화에 대한 수치해석

라자세칼* · 김태호** · 김희동†

Computational Analysis of Mitigation of Shock wave using Water Column

Jayabal Rajasekar*, Tae Ho Kim** and Heuy Dong Kim*

Abstract The interaction of planar shock wave with rectangular water column is investigated numerically. The flow phenomenon like reflection, transmission, cavitation, recirculation of shock wave, and large negative pressure due to expansion waves was discussed qualitatively and quantitatively. The numerical simulation was performed in a shock tube with a water column, and planar shock was initiated with a pressure ratio of 10. Three cases of the water column with different thicknesses, namely 0.5D, 1D, and 2D, were installed and studied. Water naturally has a higher acoustic impedance than air and mitigates the shock wave considerably. The numerical simulations were modelled using Eulerian and Volume of fluids multiphase models. The Eulerian model assumes the water as a finite structure and can visualize the shockwave propagation inside the water column. Through the volume of fluids model, the stages of breakup of the water column and mitigation effects of water were addressed. The numerical model was validated against the experimental results. The computational results show that the installation of a water column significantly impacts the mitigation of shock wave.

Key Words : Shockwave(충격파), Water Column(액주), Air-Water Interface(공기-물 경계면), Mitigation(완화), Unsteady Flow(비정상유동)

1. Introduction

Even though the interaction of shockwaves and water column is an interesting topic, very few researchers were worked on this subject⁽¹⁻⁴⁾. This

work includes shock wave propagation inside the water column, the interaction of shock at the air-water interface (interface 1), water-air interface (interface 2), the breakup of the water column into droplets, and mitigation of shock wave. In this study, different numerical models were employed to achieve desired results. Eulerian multi-phase models are used to study the shock propagation in the water column, and volume of fluids models are used to study water's breakup and mitigation behaviour⁽⁵⁻⁹⁾. Both air-water and water-air interface have a significant role in the shock wave's flow

† Department of Mechanical Engineering, Andong National University, Korea, Professor
E-mail: kimhd@anu.ac.kr

* Department of Mechanical Engineering, Andong National University, Ph.D Student

** Department of Mechanical Engineering, Andong National University, Research Professor

properties, which may be due to the acoustic impedance difference between air and water⁽¹⁰⁻¹²⁾. This topic involves various domestic and industrial applications such as rain erosion damage, atomization of the liquid jet, detonation, combustion of multi-phase mixtures, mining, military and naval applications Etc.⁽¹³⁾.

Experimental and numerical results of Sembian et al. discussed the interaction of shockwave and cylindrical water column⁽¹³⁾. In general, water has the nature to splash sideways if an external force hits it, but Sembian et al. used hydrophobic coating to fix the water column in a cylindrical shape. Numerical work by Xiang et al. presented the hollow cylindrical water column and the deformation of the water column during the interaction with the shock wave⁽¹⁴⁾. The droplet breakup modes are classified based on the Weber number⁽¹⁴⁻¹⁶⁾. Theofanous et al. reclassified it into Rayleigh Taylor piercing, shear-induced entrainment, and transition regime based on Weber number⁽¹⁷⁾. The initial stages of droplet breakup and shock propagation were studied in different numerical works⁽¹⁵⁻¹⁸⁾. Rajasekar et al. studied the effect of the equation of the state of water and air in computational simulations⁽¹⁹⁾. Also, they investigated the mitigation of shock wave due to external barriers⁽²⁰⁾. Though there are few works in this area, no computational or experimental works are available in the study related to the rectangular water column, the interface's effect, and the water column's mitigation effects. Hence in this study, the above parameters were numerically studied.

The main aim of this study is to numerically evaluate the early stage interaction of planar shock wave and rectangular water column in a higher Weber and shear stripping regime. The finite volume-based numerical technique is employed in this study. Multiphase models such as Eulerian and Volume of fluids were used to study shock wave propagation and mitigation behaviour of the water

column, respectively. The manuscript is organized as follows: numerical analysis in section 2, validation in section 3, result and discussion, and conclusion in sections 4 and 5.

2. Numerical Analysis

2.1 Governing Equations

The Reynolds number (Re) and Weber number (We) for incident shock Mach number (Ma = 3) were calculated using the following expressions:

$$Re = \frac{\rho_2 u_2 d_0}{\mu_g}, \quad We = \frac{\rho_2 u_2^2 d_0}{\sigma} \quad (1)$$

where u_2 and ρ_2 are the velocity and density of the gas behind the shock wave, μ_g is the dynamic viscosity of the gas, d_0 is the diameter of the water column, and σ is the surface tension coefficient.

The Reynolds and Weber numbers were significantly higher for incident shock Mach number (Ma=3). Hence inertial force dominates over the surface tension, which is neglected in this model. The main aim of this study is to find the interaction between incident shock wave and water column during initial timeframes, so it is a reasonable assumption to neglect surface tension at early stages⁽²¹⁻²²⁾.

With all these approximations, the flow is modelled by 2D compressible multiphase equations. The Volume of Fluids (VOF) is used to capture the movement of the shock wave interaction with the water column based on volume fraction. In this study, the Navier-Stokes equations were employed to model the flow. It expresses the conservation of mass, momentum, and energy for compressible flow along with the standard k- ϵ turbulence model that was solved. The equations were expressed as follows:

$$\begin{aligned} & \frac{\partial}{\partial t}(\rho k) + \frac{\partial}{\partial x_i}(\rho k u_i) \\ &= \frac{\partial}{\partial x_j} \left[\left(\mu + \frac{\mu_i}{\sigma_k} \right) \frac{\partial}{\partial x_j} \right] + G_k + G_b - \rho \varepsilon - Y_M \end{aligned} \quad (2)$$

and

$$\begin{aligned} & \frac{\partial}{\partial t}(\rho \varepsilon) + \frac{\partial}{\partial x_i}(\rho \varepsilon u_i) \\ &= \frac{\partial}{\partial x_j} \left[\left(\mu + \frac{\mu_i}{\sigma_\varepsilon} \right) \frac{\partial}{\partial x_j} \right] + C_{1\varepsilon} \frac{\varepsilon}{k} (G_k + C_{3\varepsilon} G_b) - C_{2\varepsilon} \rho \frac{\varepsilon^2}{k} \end{aligned} \quad (3)$$

Where G_b and G_k are the generations of turbulence kinetic energy due to the buoyancy and mean velocity gradients respectively. Y_M is the contribution of the fluctuating dilatation in compressible turbulence to the overall dissipation rate. $C_{1\varepsilon}$, $C_{2\varepsilon}$, and $C_{3\varepsilon}$ are constants. σ_k and σ_ε are the turbulent Prandtl numbers for k and ε respectively.

The ideal gas equation of state is given as follows:

$$p = (\gamma - 1) \rho e, \quad (4)$$

Where γ is constant specific heat ratio and in this case $\gamma > 1$. e is specific internal energy.

The water column was modeled using Tait's equation and it is given as follows:

$$P = (p_0 + B) \left(\frac{\rho}{\rho_0} \right)^\gamma - B \quad (5)$$

Where ρ_0 and p_0 where reference density and pressure, γ is the adiabatic index, and B is a pressure-like constant. γ and B were chosen between 6.68 and 3050 bars respectively.

2.2 Computational Domain

The computational domain is shown in Fig. 1. The domain consists of the driver (P_4) and driven

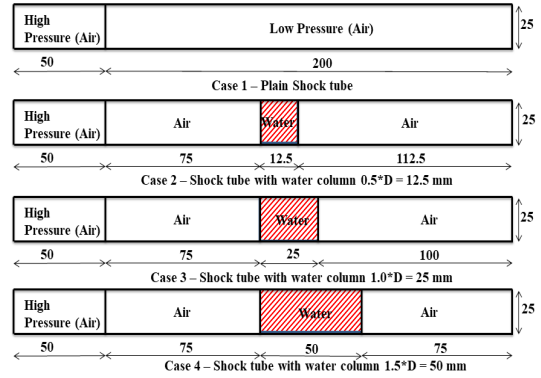


Fig. 1 Schematic diagram of the computational domain. All Dimensions are in mm.

(P_1) sections separated by the diaphragm. The driver-to-driven length ratio is 1:5, and the pressure ratio is 10:1 bar, respectively. The diameter of the shock tube is 25mm. Once the diaphragm ruptures, it creates a shock wave front due to the pressure difference between the chambers. The shock wave has a very high Mach number followed by density, pressure, and temperature jumps. In this study, a water column was introduced into the driven section of the shock tube to study the water's flow characteristics and mitigation characteristics.

As shown in Fig. 1, different water column lengths are installed in the shock tube a) Plain shock tube, b) Shock tube with water column $0.5*D$, c) Shock tube with water column $1.0*D$, d) Shock tube with water column $2.0*D$. Computational fluid dynamics simulations have been carried out in different water column domains.

2.3 Numerical Scheme

Computational simulations were carried out to find the shock wave propagation characteristics of the air-water and water-air interface and the mitigation characteristics of the water column. As the pressure ratio of the driver and driven shock tube is 10:1, once the diaphragm ruptures, the shock propagates at a relatively higher Mach

number, and corresponding Re and We numbers are relatively high. This shows that the inertial force dominates the surface tension and viscous forces. Since we mainly study the shock propagation at air-water and water-air interface, neglecting surface tension and viscosity is a reasonable assumption. Hence Eulerian Multiphase model is used to solve the governing equations for each phase. Our second aim is to find the mitigation of shockwave using a water column; since the fluids are immiscible, the Volume of fluid (VOF) is employed in this study to capture the movement of air-water and water-air interface based on volume fraction. The VOF model considers all fluids as immiscible phases and shares pressure, velocity, and temperature fields. The commercial CFD software package Ansys Fluent is used in this study⁽²³⁾.

Grid plays a vital role in determining the flow parameters at each location in a computational domain. In this study, a uniform grid was applied using commercial meshing software ANSYS ICEM CFD. The domain has been discretized equally using quadrilateral cells with a grid size of 0.625 million cells and a corresponding physical length of 0.1 mm.

3. Validation

The numerical simulation was validated against the experimental work done by Sembian et al.⁽¹³⁾. In the experimental work, Sembian et al.⁽¹³⁾ studied the wire explosion inside the shock tube without a water column. The pressure time histories were monitored at 200 mm and 240 mm from the charge using sensors. In the computational analysis, the charge was modelled using the TNT, and gauge points were fixed in the place of sensors.

Fig. 2 compares pressure time histories of numerical and experimental results. As shown in Fig. 2, the numerical results show good agreement

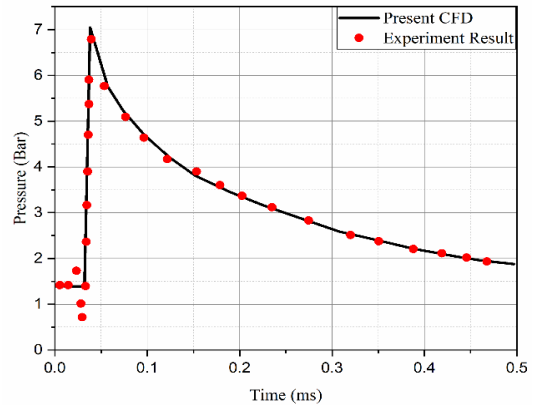


Fig. 2. Comparison of present CFD results and Experimental results⁽¹³⁾

with experimental results. The results were able to predict the pressure profiles, speed, and location of the shock wave at each sensor. A grid independence simulation was also conducted, and the above results were independent of grid size.

4. Results and Discussion

4.1 Flow Characteristics

In this study, the shock tube consists of high-pressure and low-pressure air separated by a diaphragm. Once the diaphragm breaks, the incident shock wave moves toward the water column. The incident shockwave reaches the air-water interface, and the shockwave gets reflected in the upstream region and transmitted downstream of the shock wave. The reflected and transmitted shock wave is either the shockwave/compression wave or expansion/rarefaction wave. It depends on the acoustic impedance of the impinging body. Acoustic impedance is defined as $Z=\rho c$, where ρ and c are the density and speed of sound, respectively. In this study, the shockwave hits the water, and the acoustic impedance of water is much higher than that of air ($Z_{\text{water}} \gg Z_{\text{air}}$). Hence the reflection of a shockwave is similar to that of a shockwave reflected from a solid body.

The flow was simulated using the Eulerian multiphase model in all three cases. This model is employed to visualize the shock propagation inside the water region without disturbing the structure of the water column. So, with the help of these computational techniques, the breakup of water was neglected, and able to visualize the shock wave propagation inside the water column.

As shown in Fig. 3, when the diaphragm breaks, the planar shock wave approaches and encounters the water column. At time $t = 0.145$ ms, due to the acoustic impedance of water, the shock wave reflects as a compression wave along the upstream and transmits as a shockwave with a considerably higher magnitude. Hence the shockwave transmits into the water column and reaches the water-air interface at $t=0.15$ ms. Here again, the acoustic impedance of water plays a significant role. Due to that, transmitted shock reflects as an expansion wave at the water-air interface. The shockwave expansion inside the water region results in negative pressure in that region, which is otherwise said to be cavitation.

Negative pressure means the absolute pressure drops below 0 for a few milliseconds. Naturally, liquid substances have considerable cohesive forces and withstand higher tensile stress or negative pressures. As per Classical Nucleation Theory (CNT), due to its strong, cohesive nature, water

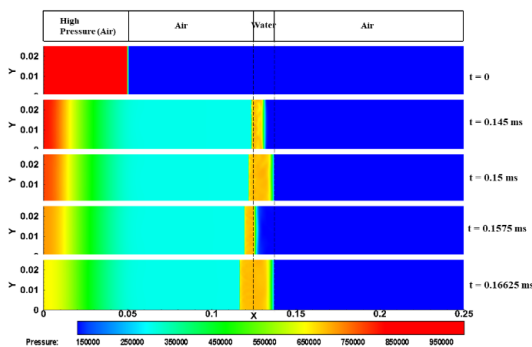


Fig. 3. Pressure contour of case 2 (water column = 12.5 mm)

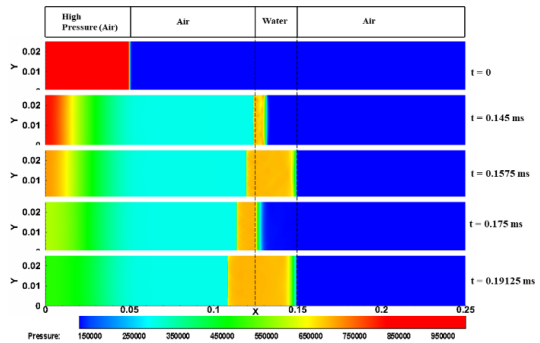


Fig. 4. Pressure contour of case 3 (water column = 25 mm)

can withstand a negative pressure of around -100MPa ⁽²⁴⁾. The pressure due to tension stress in water was referred to in this study as negative pressure. Hence due to this reason, the cavitation due to reflected wave is very minimal and neglected. This shockwave is trapped inside the water column, moves back and forth, and attenuates gradually.

In Fig. 4, the flow physics of shockwave propagation inside the water column remains the same as in case 1.

Fig. 4, at time $t=0.1575$ ms, clearly shows that the shock wave propagation inside the water is faster than that of the reflected wave at the air-water interface. This is due to the acoustic impedance difference between air and water. The acoustic impedance of water and air at a pressure of 1 atm and temperature of 15°C is $1.5 \cdot 10^6 \text{ kg m}^{-2} \text{ s}^{-1}$ and $410 \text{ kg m}^{-2} \text{ s}^{-1}$, respectively. Due to this reason, the shock propagation inside the water column is around four times higher than that of shock propagation in the air region.

As shown in Fig. 5, the shockwave enters the air-water interface at time $t=0.145$ ms. It reflects at interface 1 and propagates inside the water column at a higher pace. It reaches the water-air interface at time $t=0.175$ ms. Here water tries to transmit in the air region and reflect in the water column. Again, it reaches the air-water interface at time $t=0.2075$ ms. This time it transmits at interface 1

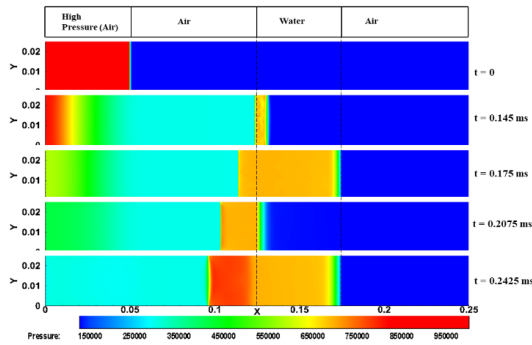


Fig. 5. Pressure contour of case 4 (water column = 50 mm)

and reflects in the water column at $t=0.2425$ ms. At this point, the reflected and transmitted shock combine, and shock pressure in that region also increases significantly, as shown in Fig. 5. Hence the shock wave was trapped inside the water column and moved back and forth inside the column. It results in the attenuation of the shock wave. On the other hand, it results in the breakup of the water column.

4.2 Mitigation Characteristics

In this study, the computation was modelled using the volume of fluids (VOF). VOF method of simulation is used to study the break-up physics and mitigation characteristics of water.

Fig. 6 shows the phase change diagram of case 2. It also shows the pressure contour diagram at time $t=0$ for better visualization. Once the diaphragm

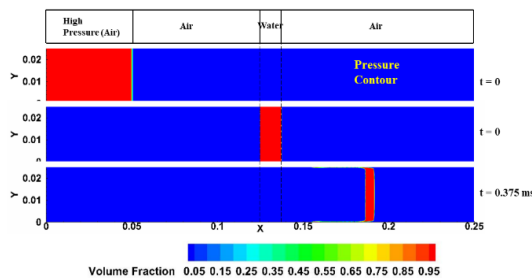


Fig. 6. Phase change diagram of case 2 (water column = 12.5 mm)

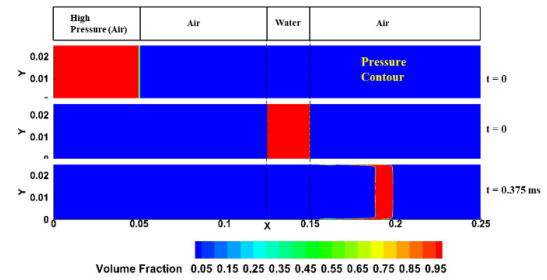


Fig. 7. Phase change diagram of case 3 (water column = 25 mm)

breaks and the shock reach the air-water interface, the maximum pressure from the air region transmit inside the water column. Due to high pressure from the shock wave, water cannot retain such tensile force, and it starts to deform longitudinally and break up successively, as shown in Fig. 6 at time $t=0.375$ ms.

In Fig. 7, the water column has a length of $1.0 \cdot D$, so the thickness of the water column is 25mm. As the thickness of the water column was higher, it could withstand the force given by the shockwave for a few more milliseconds. Then the deformation of shock starts, and the breakup of water follows up. The water column moves along with the direction of the shock wave, and the thickness of the water column is reduced significantly due to flow field variables and the water breakup into smaller droplets on both the sides of the wall, as shown in Fig. 7.

As shown in Fig. 8, the thickness of the water

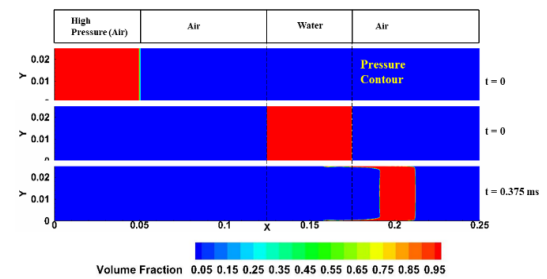


Fig. 8. Phase change diagram of case 4 (water column = 50 mm)

column is 50 mm. The maximum pressure used in this study is 10 bar. As the shockwave impacts the water column, due to the thickness of the water column initially, it can withstand the shock. The shockwave moves back and forth as time proceeds, and the breakup process begins. Due to the resistance of the water column, the deformation and break up of water into droplets are considerably small. Thereby the shockwave was attenuated significantly.

4.3 Wave Diagram

As shown in Fig. 9, the wave diagram helps study the shock wave propagation inside the shock tube. At the distance of 50mm, the planar shock initiated and propagated downstream as a shockwave and upstream as an expansion wave. When the shock reaches interface 1 (i.e. air-water interface), the shock wave transmits and propagates at a higher speed. The other part of the shock reflects in the air region and propagates at a comparably lower pace. The transmitted shock reaches the water-air interface, and again it transmits at interface 2 and reflects inside the water column, as shown in the Fig. . This time the reflected shock is a rarefaction wave due to the acoustic impedance difference between air and water. The transmitted shock is very weak and

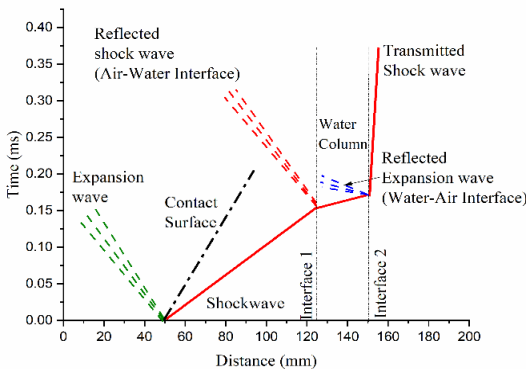


Fig. 9. Wave diagram of case 3 (water column= 25mm)

attenuated significantly due to the presence of a water column.

Comparison of Results

Fig. 10 shows the comparison of all cases of the water column. For calculating the percentage reduction of shock pressure, the monitoring line was positioned before and after the water column at a distance of 100 mm and 200 mm, respectively. The area-weighted average of pressure values was computationally analyzed and monitored. The graph clearly shows that the mitigation of shockwaves is directly proportional to water column thickness.

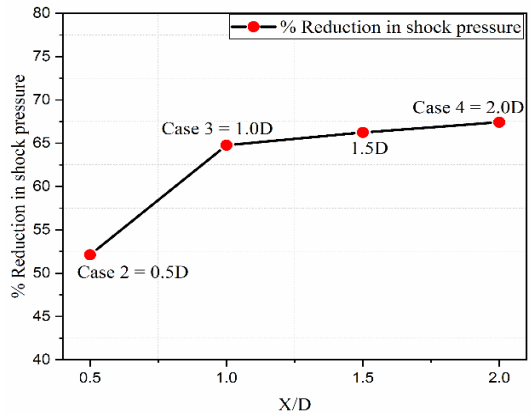


Fig. 10. Percentage reduction of shock pressure for different water column thickness

As in case 2, the percentage reduction in shock pressure is 52.12%. Cases 3 and 4 are 64.76% and 67.43%, respectively. Hence for the pressure ratio of 10 bar, the water column thickness of 25 mm mitigates the shock wave significantly, and a further increase in water column thickness shows a very minimal increase in the percentage reduction of shock pressure, as shown in Fig. 10.

5. Conclusion

This study aims to investigate the interaction of planar shock wave with rectangular water column

and numerically calculates the mitigation effect of different water column thicknesses. For studying the shock propagation inside water, the water column was modelled using the Eulerian multiphase approach, so it neglects the deformation characteristics of water. Hence in all three cases, the shockwave approaches the water column and impinges at the air-water interface. The shock wave transmits into the water column and reflects in the air region. The transmitted shock propagates in the water column and reaches the water-air interface. Due to the acoustic impedance difference between air and water, the shock wave reflects and transmits as a weak shock wave inside the water column. Hence the shock moves between both interfaces and dissipates abruptly.

For studying the effect of mitigation, the water column was modelled using the volume of fluids. In all three cases, once the planar shock interacts with the water column, the thickness of the water shrinks due to the strength of the shock wave. The pressure of the shockwave was monitored at two locations and compared for all three cases. The water column thickness of the 1D case shows a significant impact, and a further increase in thickness gives minimal impact in mitigation. Hence the results show that the water column plays a significant role in the mitigation of shock wave.

Acknowledgment

This work was supported by a Research Grant from Andong National University.

References

- 1) Igra D and Takayama K, 2021, Study of Two Cylindrical Water Columns Subjected to Planar Shock Wave Loading. ASME International Mechanical Engineering Congress and Exposition, Proceedings (IMECE), Vol. 2000-R, pp.15–20.
- 2) Chen H and Liang S. M, 2008, Flow visualization of shock/water column interactions. Shock Waves, Vol.17, pp. 309–321.
- 3) Igra D and Takayama K, 2001, Numerical simulation of shock wave interaction with a water column. Shock Waves, Vol. 11, pp. 219–228.
- 4) Yoshida T and Takayama K, 1990, Interaction of liquid droplets with planar shock waves. Journal of Fluids Engineering, Transactions of the ASME, Vol. 112, pp.481–486.
- 5) Liverts M, Ram O, Sadot O, Apazidis N and Ben-Dor G, 2015, Mitigation of exploding-wire-generated blast-waves by aqueous foam. Physics of Fluids, Vol. 27.
- 6) Wan Q, Deiterding R and Eliasson V, 2019, Numerical investigation of shock wave attenuation in channels using water obstacles. Multiscale and Multidisciplinary Modeling, Experiments and Design, Vol.2, pp. 159–173.
- 7) Jourdan G, Biamino L, Mariani C, Blanchot C, Daniel E, Massoni J, Houas L, Tosello R and Praguine D, 2010, Attenuation of a shock wave passing through a cloud of water droplets. Shock Waves, Vol.20, pp. 285–296.
- 8) Adiga K. C, Willauer H. D, Ananth R, and Williams F. W, 2009, Implications of droplet breakup and formation of ultra fine mist in blast mitigation. Fire Safety Journal, Vol. 44, pp. 363–369.
- 9) Williams F. W, 2002, Blast Mitigation Using Water.
- 10) Rossano V and De Stefano G, 2021, Computational Evaluation of Shock Wave Interaction with a Cylindrical Water Column.
- 11) James J. K and Kim H. D, 2019, Multiple Shock Waves and its Unsteady Characteristics in Internal Flows. ASME-JSME-KSME 2019 8th Joint Fluids Engineering Conference, AJKFluids 2019, Vol.1.
- 12) Igra D and Sun M, 2010, Shock-water column interaction, from initial impact to fragmentation

- onset. *AIAA Journal*, Vol. 48, pp. 2763–2771.
- 13) Sembian S, Liverts M, Tillmark N and Apazidis N, 2016, Plane shock wave interaction with a cylindrical water column. *Physics of Fluids*, Vol.28.
 - 14) Xiang G and Wang B, 2017, Numerical study of a planar shock interacting with a cylindrical water column embedded with an air cavity. *Journal of Fluid Mechanics*, pp.825–852.
 - 15) Pilch M and Erdman C. A, 1987, Use of breakup time data and velocity history data to predict the maximum size of stable fragments for acceleration-induced breakup of a liquid drop. *International Journal of Multiphase Flow*, Vol.13, pp. 741–757.
 - 16) Wierzbna A and Takayama K, 1988, Experimental investigation of the aerodynamic breakup of liquid drops. *AIAA Journal*, Vol.26, pp. 1329–1335.
 - 17) Theofanous T. G, Li G. J and Dinh T. N, 2004, Aerobreakup in rarefied supersonic gas flows. *Journal of Fluids Engineering, Transactions of the ASME*, Vol. 126, pp. 516–527.
 - 18) Hsiang L. P and Faeth G. M, 1992, Near-limit drop deformation and secondary breakup. *International Journal of Multiphase Flow*, Vol.18, pp. 635–652.
 - 19) Rajasekar J, Kim T. H and Kim H. D, 2020, Visualization of shock wave propagation due to underwater explosion. *Journal of Visualization*, Vol. 23, pp. 825–837.
 - 20) Rajasekar J, Yaga M and Kim H. D, 2022, Numerical prediction on the mitigation of shock wave using geometric barriers. *Journal of Visualization* Vol.22, pp. 1–14.
 - 21) Igra D and Takayama K, 2003, Experimental investigation of two cylindrical water columns subjected to planar shock wave loading. *Journal of Fluids Engineering, Transactions of the ASME*, Vol.125, pp.325–331.
 - 22) Chauvin A, Jourdan G, Daniel E, Houas L and Tosello R, 2011, Experimental investigation of the propagation of a planar shock wave through a two-phase gas-liquid medium. *Physics of Fluids*, Vol. 23, pp. 1–14.
 - 23) Launder and Spalding, 2013, *ANSYS Fluent User' s Guide* 15.0.
 - 24) Gabi Ben-Dor, 2007, *Shock Wave Reflection Phenomena*. Gabi Ben-Dor, 2007, *Shock Wave Reflection Phenomena*.